THE JOURNAL OF PHYSICAL CHEMISTRY Letters
Cite This: J. Phys. Chem. Lett. 2019, 10, 7195−7199
Letter
pubs.acs.org/JPCL

Attractive Interaction between Fully Charged Lipid Bilayers in a Strongly Confined Geometry

Tetiana Mukhina,[†,‡] Arnaud Hemmerle,[†,⊥] Valeria Rondelli,[§] Yuri Gerelli,[‡] Giovanna Fragneto,[‡] Jean Daillant,[∥] and Thierry Charitat*[,†]

[†]UPR 22/CNRS, Institut Charles Sadron, Université de Strasbourg, 23 rue du Loess, BP 84047, 67034 Strasbourg Cedex 2, France
[‡]Institut Laue-Langevin, 71 av. des Martyrs, BP 156, 38042 Grenoble Cedex, France
[§]Dipartimento di Biotecnologie Mediche e Medicina Traslazionale, Universitá degli Studi di Milano, LITA, Via F.lli Cervi 93, 20090 Segrate, Italy
[∥]Synchrotron SOLEIL, L'Orme des Merisiers, Saint-Aubin, BP 48, F-91192 Gif-sur-Yvette Cedex, France

Supporting Information

ABSTRACT: We investigate the interaction between highly charged lipid bilayers in the presence of monovalent counterions. Neutron and X-ray reflectivity experiments show that the water layer between like-charged bilayers is thinner than for zwitterionic lipids, demonstrating the existence of counterintuitive electrostatic attractive interaction between them. Such attraction can be explained by taking into account the correlations between counterions within the Strong Coupling limit, which falls beyond the classical Poisson−Boltzmann theory of electrostatics. Our results show the limit of the Strong Coupling continuous theory in a highly confined geometry and are in agreement with a decrease in the water dielectric constant due to a surface charge-induced orientation of water molecules.

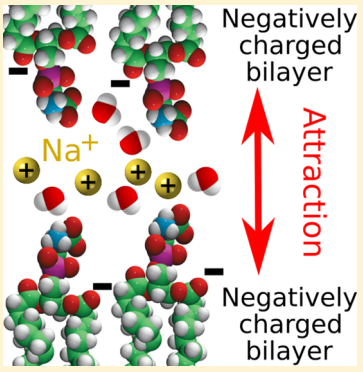

Understanding electrostatic interactions between charged confined surfaces across aqueous electrolytes is important in many fundamental and applied research areas. For example, these interactions are crucial for controlling the properties of a colloidal suspension.[1,2] In biology, many specific functions of cell membranes strongly depend on electrostatic interactions, such as interactions with biomolecules, membrane adhesion, and cell−cell interactions.[3] Electrostatic interactions between charged surfaces in water (dielectric permittivity ε_w) have been widely investigated both theoretically and experimentally in the case of two infinitely large planar walls with a uniform surface charge density σ_s and positively charged counterions of charge qe, where q is the counterion valence, at temperature T. The Bjerrum length $l_B = e^2/4\pi\varepsilon_w k_B T \sim 0.7$ nm compares the electrostatic interaction between counterions to their thermal energy. The Gouy−Chapman length $b=1/(2\pi q l_B \sigma_S)$ characterizes the thickness of the diffuse counterion layer close to the membrane, without added salt, as a function of charge density σ_s. The coupling constant $\Xi = l_B q^2/b = 2\pi q^3 l_B^2 \sigma_s$ quantifies the competition between the counterion−counterion interaction and thermal agitation $k_B T$. For low coupling constant values, i.e., $\Xi \ll 1$, ion correlations are negligible and the distribution of ions can be evaluated by the Poisson−Boltzmann (PB) theory in the mean-field approximation.[3] PB theory predicts a repulsive pressure between similarly charged surfaces and has been confirmed by numerous experiments (for a review, see ref 2). For high coupling constant values, i.e., $\Xi \gg 1$, the PB theory fails and correlations between ions start to be non-negligible. Indeed, strong coupling (SC) theory and numerical simulations were developed to describe electrostatic interactions in this regime,[4−10] showing that identically charged plates can attract each other for large coupling parameters $\Xi \geq 20$. Most experimental investigations of the SC limit have been carried out using divalent counterions to increase the coupling constant Ξ. Under such conditions, an attraction, in good agreement with the strong coupling limit, was observed between mica surfaces,[11] between lamellar systems,[12] and between two charged vesicles.[13] Recently, surface force apparatus experiments were performed to measure the compressibility modulus of charged membranes in the presence of monovalent counterions. For large water separation distances (d > 5 nm), where effects related to the structure of water are negligible, a good agreement with weak coupling corrections, still in the repulsive regime ($\Xi \sim 3$), was obtained.[14] In this paper, we explore the poorly understood limit of strong confinement, where continuous theories reach

Received: September 24, 2019
Accepted: November 3, 2019
Published: November 4, 2019

DOI: 10.1021/acs.jpclett.9b02804
J. Phys. Chem. Lett. 2019, 10, 7195−7199

their limits, as already highlighted numerically[15] and first evidenced by pioneering works on black films.[16]

Samples consisted of two supported bilayers deposited consecutively on ultraflat silicon substrates[17−19] (see the inset of Figure 1). Highly charged double bilayers were prepared

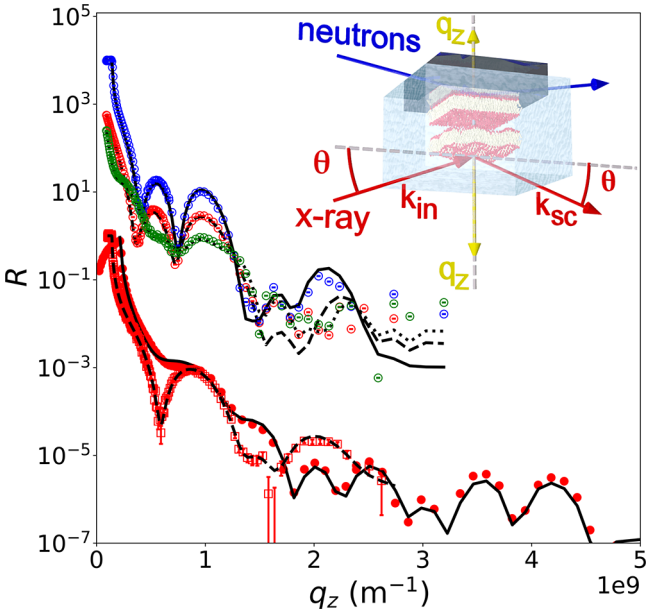

Figure 1. Neutron reflectivity (NR, empty red squares) and X-ray reflectivity (XRR, filled red circles) for double DPPS bilayers at 40 °C (in the gel phase) (bottom). Dashed and solid lines are the best fits corresponding to the SLD profiles reported in Figure 2. NR data in three different contrasts (top): (empty blue circles) in D_2O shifted by 4 decades for the sake of clarity, (empty red circles) in SiMW, and (empty green circles) in H_2O for DPPS triple bilayers at 25 °C.

using DPPS [1,2-dipalmitoyl-*sn*-glycero-3-phospho-L-serine (sodium salt), Avanti Polar Lipids, Alabaster, AL; main transition temperature T_m = 54 °C]. This system is hereafter denoted $DPPS_2$-$DPPS_2$. Zwitterionic double bilayers were prepared using DSPC (1,2-dipalmitoyl-*sn*-glycero-3-phosphocholine, Avanti Polar Lipids; main transition temperature T_m = 55 °C), and the resulting system is hereafter denoted $DSPC_2$-$DSPC_2$. A double asymmetric bilayer, denoted DPPC/DPPS-DPPS/DPPC, and a triple DPPS bilayer, denoted $DPPS_2$-$DPPS_2$-$DPPS_2$, were also investigated. All of the samples were prepared using the Langmuir−Blodgett (LB) and Langmuir−Schaefer (LS) deposition techniques (see more details in the Supporting Information).

We have combined neutron reflectivity (NR) and X-ray reflectivity (XRR) to characterize with a high resolution (∼0.1 nm) the structure of double bilayers. NR measurements were performed on the D17 reflectometer[20] at the Institut Laue-Langevin (ILL, Grenoble, France).

The neutron beam was configured to illuminate the silicon substrate through the interface at which the sample was deposited. To apply the contrast variation method[21] to reduce the ambiguities of the fits,[17,22] each system was measured against three different water solutions, namely, 100% H_2O [scattering length density (SLD) of -0.56×10^{-6} Å^{-2}], silicon-match water (SiMW, i.e., 62% H_2O and 38% D_2O by volume; SLD = 2.07×10^{-6} Å^{-2}), and 100% D_2O (SLD = 6.35×10^{-6} Å^{-2}). XRR experiments were performed at the European Synchrotron Radiation Facility (ESRF, French CRG-IF, Grenoble, France) using a 27 keV X-ray beam (wavelength λ = 0.0459 nm). For both NR and XRR, specular reflectivity $R(q_z)$ is defined as the ratio between the specularly reflected and incoming intensities of a beam. $R(q_z)$ is expressed as a function of the wave vector transfer, $q_z = 4\pi/\lambda \sin\theta$, in the direction perpendicular to the sample surface, where θ is the grazing angle of incidence and reflection (see Figure 1). NR data were fitted with the AURORE software according to a discrete SLD profile,[23] while XRR data were fitted using a hybrid Gaussian continuous SLD profile (see refs 18 and 24).

Figure 1 shows NR and XRR data for $DPPS_2$-$DPPS_2$, and the best fits corresponding to the SLD profiles are shown in Figure 2. Both NR and XRR profiles are in good quantitative

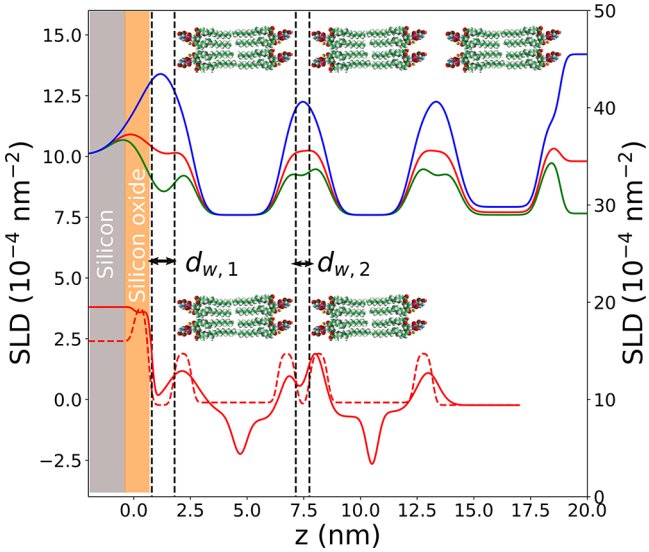

Figure 2. SLD for NR (solid lines, left axis) and XRR (dashed lines, right axis) profiles corresponding to the best fits reported in Figure 1: (bottom) $DPPS_2$-$DPPS_2$ at 40 °C and (top) $DPPS_2$-$DPPS_2$-$DPPS_2$ at 25 °C in D_2O, SiMW, and H_2O contrast (shifted by 8×10^{-4} nm^{-2} for the sake of clarity).

agreement. We define the water thicknesses between the substrate and the first bilayer ($d_{w,1}$) and between the two bilayers ($d_{w,2}$) by the distance between inflection points in the SLD profiles (see the dashed line in Figure 2). We have investigated the variation of $d_{w,1}$, the thickness of the water layer between the silicon oxide and the bilayer, and $d_{w,2}$, the interbilayer water thickness, as a function of temperature (see Figure 3a,b) and as a function of Debye length $l_D = (\varepsilon_w k_B T/2e^2 c)^{1/2}$ with the change in NaCl concentration c (0.01−0.3 M) (see Figure 4a,b) for $DPPS_2$-$DPPS_2$ and DSPC/DPPS-DPPS/DSPC samples. The obtained result was compared to our previous work on $DSPC_2$-$DSPC_2$in the absence and presence of NaCl (0.5 M).[19,25]

As expected, $d_{w,1}$ is larger when the first bilayer is charged ($d_{w,1} \sim 1.0 \pm 0.1$ nm for $DPPS_2$-$DPPS_2$) than when it is composed of zwitterionic phospholipids ($d_{w,1} \sim 0.6 \pm 0.1$ nm for $DSPC_2$-$DSPC_2$). $d_{w,1}$ is mainly controlled by the weak electrostatic repulsive interaction between the first monolayer and the silicon oxide layer of the substrate that is negatively charged, because of the experimental conditions and the surface treatment prior to the deposition (see more details in the Supporting Information). With the exception of a small variation around the transition temperature, within the

DOI: 10.1021/acs.jpclett.9b02804
J. Phys. Chem. Lett. 2019, 10, 7195−7199

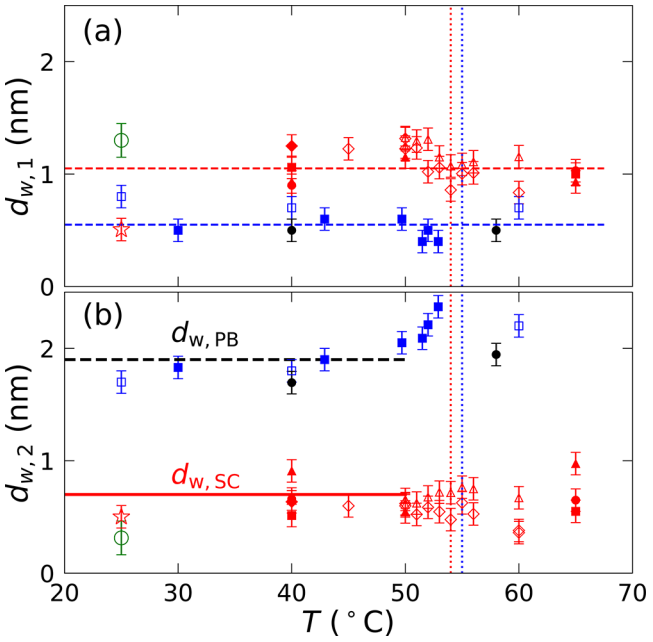

Figure 3. (a) $d_{w,1}$ and (b) $d_{w,2}$ obtained from NR (empty symbols) and XRR (filled symbols): $DSPC_2$-$DSPC_2$ with (●) and without salt (filled and empty blue squares), $DPPS_2$-$DPPS_2$ double bilayer (XRR, four different samples, red filled squares, triangles, circles, and diamonds; NR, two different samples, empty red triangles and diamonds), $DPPS_2$-$DPPS_2$-$DPPS_2$ (empty red circles), and a DSPC/DPPS-DPPS/DSPC double asymmetric bilayer (empty red star). (a) Dashed lines are guides for the eye corresponding to average values. (b) The black dashed line (---) corresponds to a $d_{w,vdW}$ of 1.9 nm, and the red solid line corresponds to a $d_{w,SC}$ of 0.7 nm. Dotted lines correspond to the gel to fluid transition temperature for DSPC (blue dotted line) and DPPS (red dotted line) bilayers.

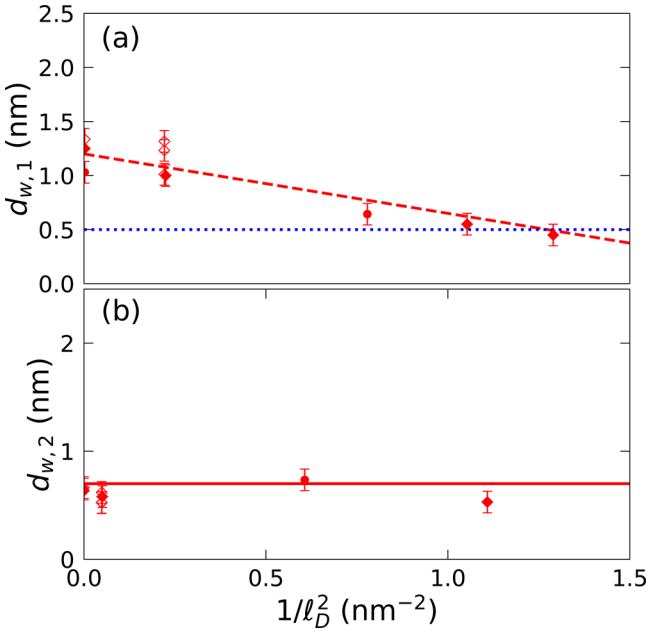

Figure 4. (a) $d_{w,1}$ and (b) $d_{w,2}$ vs $1/l_D^2$ (same notations as in Figure 3). (a) The blue dotted line corresponds to a $d_{w,1}$ of 0.5 nm, the average value for the DSPC case, and the red dashed line to the osmotic pressure effect. (b) The red solid line corresponds to strong coupling theory $d_{w,SC}$ = 0.7 nm.

resolution limit of the techniques, we did not observe a significant variation of $d_{w,1}$ with temperature. This shows that the entropic contributions related to membrane fluctuations are negligible. Finally, we observed that $d_{w,1}$ decreases as the salt concentration increases (see Figure 4a), reaching values close to those observed for the $DSPC_2$-$DSPC_2$ case ($d_{w,1} \sim 0.5$ nm). This is in good qualitative agreement with an osmotic pressure effect as described in ref 26 (see also the Supporting Information).

We now discuss the case of $d_{w,2}$ (see Figure 3b). As in the case of $d_{w,1}$, $d_{w,2}$ values obtained from NR and XRR data are in good agreement. In the case of $DPPS_2$-$DPPS_2$ charged systems (red symbols in Figure 3b), we observe that $d_{w,2}$, of the order of $\simeq 0.6 \pm 0.1$ nm, is smaller than in the case of the zwitterionic $DSPC_2$-$DSPC_2$ systems, for which $d_{w,2} \simeq 1.8-2.5$ nm (blue and black symbols). Contrary to the case of zwitterionic lipids, we did not observe variations of $d_{w,2}$ with temperature, indicating that entropic contributions related to membrane fluctuations are negligible. The decrease in $d_{w,2}$ in the fully charged systems clearly indicates that the attractive contribution to the interaction potential is increased in the case of two highly like-charged membranes. We exploited this result to deposit, by means of the LB technique, up to five DPPS monolayers (see more details in the Supporting Information), leading to a triple bilayer system [$DPPS_2$-$DPPS_2$-$DPPS_2$ (see NR data in Figure 1)]. The corresponding SLD profiles, shown in Figure 2, demonstrate the high quality and structural integrity of all bilayers. If zwitterionic molecules such as phosphocholine are used, the deposition of more than three successive monolayers by LB is not possible. Trying to deposit a fourth monolayer usually leads to the partial removal of the third one (see the Supporting Information). $DPPS_2$-$DPPS_2$-$DPPS_2$ was also used to quantify attractive interactions between bilayers that are far from the solid substrate. In this case, the interbilayer water thickness $d_{w,2}$ was found to be constant (0.3 ± 0.2 nm), demonstrating that the substrate has an only minor influence on the deposition after the first monolayer. The role of electrostatic interactions is confirmed by complementary experiments on asymmetric sample DSPC/DPPS-DPPS/DSPC for which we obtained a $d_{w,2}$ of $\simeq 0.5 \pm 0.1$ nm, a value in agreement with those obtained for the $DPPS_2$-$DPPS_2$ samples (see Figure 3b). Finally, an increase in NaCl concentration in the solution has a negligible effect on the value of $d_{w,2}$, as clearly evidenced in Figure 4b.

To compare our experimental results with existing theoretical models, we have to take into account the different contributions to the interactions between adjacent bilayers. First, the short-range hydration repulsion is described by a potential $U_{hyd} = P_h\lambda_h \exp(-d_w/\lambda_h)$ with a hydration pressure P_h of 4×10^9 Pa and a decay length λ_h of 0.1–0.2 nm. We model the van der Waals attractive contribution as $U_{vdW} = -H/12\pi(d_w + 2d_{head})$ with the Hamaker constant H of 5.3×10^{-21} J and a head thickness d_{head} of ~0.5 nm. Finally, as described in our previous work,[19] the small amount of charges due to the amphoteric character of the phosphatidylcholine group ($\sigma \sim 0.001$ e/nm^2) leads to a weak electrostatic repulsion corresponding to the ideal gas limit of the mean-field PB theory $U_{PB}(z) = -2k_BT\sigma_S \log z$.[3] In the gel phase, neglecting the entropic contribution, the minimization of $U_{vdW}(z) + U_{hyd}(z) + U_{PB}(z)$, leads to an equilibrium value for water thickness $d_{w,PB}$ of $\simeq 1.9$ nm (black dashed line in Figure 3b). Such a value is in good agreement with those obtained for a $DSPC_2$-$DSPC_2$ system in the gel phase. As demonstrated in

DOI: 10.1021/acs.jpclett.9b02804
J. Phys. Chem. Lett. 2019, 10, 7195–7199

our previous work,[19] the increase in $d_{w,2}$ close to the gel−fluid transition shown in Figure 3b is described well by taking into account the entropic contribution and electrostatic repulsion in the framework of PB theory.

For DPPS double and triple bilayers, the entropic contribution is clearly negligible, as we observe no significant variation in $d_{w,2}$ with temperature. With regard to electrostatic interaction between charged surfaces, the area per molecule of DPPS can be estimated to be equal to 0.55 nm^2.[27] At pH 5−6, taking into account the respective pK_a of the phosphate, ammonium, and carboxylate groups,[28] we obtain a charge density σ of ∼0.8−1.5 e/nm^2. By estimating the coupling constant with an ε_w of ≃80ε_0, we obtain a Ξ of ≃2.5−4, which is outside the attractive zone described by the SC theory[5,9] (see the red area in Figure 5). In this limit, using realistic

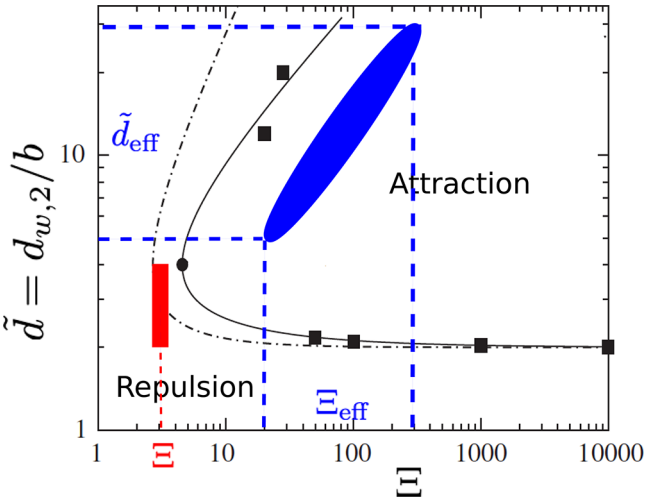

Figure 5. Phase diagram showing attraction and repulsion regimes in terms of the rescaled water thickness $\tilde{d} = d_{w,2}/b$ and as a function of coupling constant Ξ (figure adapted from ref 9). The dashed−dotted line is the original virial strong coupling theory from ref 5, and black squares are the Monte Carlo simulation data from ref 6. The solid line corresponds to the Wigner strong coupling theory from ref 9. Our experiments correspond to the red area using an ε_w of 80ε_0 ($\Xi \sim 2.5$−4; $\tilde{d} \sim 2$−4) and to the blue one, taking into account renormalization induced by water orientation ($10 \le \varepsilon_w \le 30 \Leftrightarrow 20 \le \Xi_{eff} \le 300$, $5 \le \tilde{d}_{eff} \le 30$).

values of P_h, λ_h, and H, it is not possible to access equilibrium values of $d_{w,2}$ of <1.5 nm. In such a strongly confined limit, the rotational degrees of freedom of water dipoles are expected to be frozen near surfaces, inducing a strong decrease in dielectric permittivity. Fumagalli et al.[29] experimentally demonstrated the presence of a layer that was two to three interfacial molecules thick with an ε_w of ∼2ε_0, a value close to the limit for water at optical frequencies ($\varepsilon_w \sim 1.8\varepsilon_0$). Because $\Xi \sim 1/\varepsilon^2$, this leads to a strong increase in the coupling constant. Recently, using water-explicit numerical simulations of decanol bilayers with variable charge density, Schlaich et al.[15] demonstrated that an attractive behavior can appear at a moderate surface density (∼0.77 e/nm^2; $\Xi \sim 3$), a value close to the lowest estimation of the charge density in our experiments. Their numerical results are in good agreement with an effective coupling constant Ξ_{eff} of ∼20, corresponding to a decrease in ε_w to 30. For the upper limit of charge density (∼1.5 e/nm^2), we can extrapolate an effective dielectric constant on the order of 10. The blue area in Figure 5 gives the corresponding effective values of Ξ_{eff} ($10 < \Xi_{eff} < 300$) and $\tilde{d}_{eff}$ ($5 < \tilde{d}_{eff} < 15$), taking into account the effective dielectric constant. It is clear that our experiments fall in the attractive regime, described well by SC theory where it is valid to use the analytical expression for the electrostatic pressure $P_{SC} = 2\pi l_B \sigma_S^2 (2b/z - 1) k_B T$.[5,8] The decrease in ε_w also induced a decrease in the Hamaker constant by 1 order of magnitude,[30] and it is possible to neglect the van der Waals interactions compared to the SC term. By minimizing the potential $U(z)$

$$U(z) = U_{vdW}(z) + U_{hyd}(z) - 2\pi l_B b \sigma_S^2 k_B T \left[2 \log\left(\frac{z}{b}\right) - \frac{z}{b}\right] \quad (1)$$

we obtain an equilibrium value of $d_{w,SC}$ of 0.7 nm, in very good agreement with our experimental data as shown in Figures 3b and 4b.

Electrostatic interactions between highly charged double bilayers, in the presence of monovalent counterions and in strong confinement, have been investigated by measuring the equilibrium distance between like-charged bilayers. In a consistent set of experimental data obtained on a model system close to an ideal theoretical configuration (planar geometry, negligible fluctuations), we have demonstrated the presence of an attractive electrostatic interaction, which is in contradiction to continuous theories. Our results are in agreement with recent water-explicit numerical simulations[15] predicting that ion correlations can have tremendous effects even for moderate surface charge densities in the presence of monovalent counterions. The obtained results provide a deeper understanding of electrostatic interactions in strong confinement beyond the continuous models, where the discrete nature of charges must be taken into account explicitly.

■ ASSOCIATED CONTENT

Supporting Information

The Supporting Information is available free of charge on the ACS Publications website at DOI: 10.1021/acs.jpclett.9b02804.

Detailed description of sample preparation and data analysis and detailed description of the osmotic pressure effect (PDF)

■ AUTHOR INFORMATION

Corresponding Author

*E-mail: thierry.charitat@ics-cnrs.unistra.fr. Phone: +123 (0) 123 4445556. Fax: +123 (0)123 4445557.

ORCID

Yuri Gerelli: 0000-0001-5655-8298

Thierry Charitat: 0000-0003-3167-6495

Present Address

⊥A.H.: Synchrotron SOLEIL, L'Orme des Merisiers, Saint-Aubin, BP 48, F-91192 Gif-sur-Yvette Cedex, France.

Notes

The authors declare no competing financial interest.

■ ACKNOWLEDGMENTS

The authors thank L. Malaquin and S. Micha for assistance during the experiments and P. Kékicheff, A. Johner, C. Loison, and R. Netz for fruitful discussions. Awarded beamtime at the

DOI: 10.1021/acs.jpclett.9b02804
J. Phys. Chem. Lett. 2019, 10, 7195−7199

ILL (10.5291/ILL-DATA.EASY-341) and at the ESRF is gratefully acknowledged. Support from the Labex NIE 11-LABX-0058-NIE (Investissement d'Avenir programme ANR-10- IDEX-0002-02) and PSCM facilities at the ILL for sample preparation is gratefully acknowledged. T. Mukhina tanks ILL for a PhD grant. The open access fee was covered by FILL2030, a European Union project within the European Commission's Horizon 2020 Research and Innovation programme under grant agreement N°731096.

REFERENCES

(1) Norrish, K.; Quirk, J. P. Crystalline Swelling of Montmorillonite: Use of Electrolytes to Control Swelling. *Nature* **1954**, *173*, 255−256.
(2) Belloni, L. Colloidal interactions. *J. Phys.: Condens. Matter* **2000**, *12*, R549−R587.
(3) Andelman, D. Structure and Dynamics of Membranes. In *Handbook of Biological Physics*; Lipowsky, R., Sackmann, E., Eds.; North-Holland, 1995; Vol. *1*, pp 603−642.
(4) Rouzina, I.; Bloomfield, V. A. Macroion attraction due to electrostatic correlation between screening counterions 0.1. Mobile surface-adsorbed ions and diffuse ion cloud. *J. Phys. Chem.* **1996**, *100*, 9977−9989.
(5) Netz, R. Electrostatistics of counter-ions at and between planar charged walls: From Poisson-Boltzmann to the strong-coupling theory. *Eur. Phys. J. E: Soft Matter Biol. Phys.* **2001**, *5*, 557−574.
(6) Moreira, A. G.; Netz, R. R. Binding of Similarly Charged Plates with Counterions Only. *Phys. Rev. Lett.* **2001**, *87*, 078301.
(7) Moreira, A.; Netz, R. Simulations of counterions at charged plates. *Eur. Phys. J. E: Soft Matter Biol. Phys.* **2002**, *8*, 33−58.
(8) Naji, A.; Jungblut, S.; Moreira, A. G.; Netz, R. R. Electrostatic interactions in strongly coupled soft matter. *Phys. A* **2005**, *352*, 131−170.
(9) Samaj, L.; Trizac, E. Counterions at Highly Charged Interfaces: From One Plate to Like-Charge Attraction. *Phys. Rev. Lett.* **2011**, *106*, 078301.
(10) Samaj, L.; Trulsson, M.; Trizac, E. Strong-coupling theory of counterions between symmetrically charged walls: from crystal to fluid phases. *Soft Matter* **2018**, *14*, 4040−4052.
(11) Kékicheff, P.; Marcelja, S.; Senden, T. J.; Shubin, V. E. Charge reversal seen in electrical double layer interaction of surfaces immersed in 2:1 calcium electrolyte. *J. Chem. Phys.* **1993**, *99*, 6098−6113.
(12) Khan, A.; Joensson, B.; Wennerstroem, H. Phase equilibria in the mixed sodium and calcium di-2-ethylhexylsulfosuccinate aqueous system. An illustration of repulsive and attractive double-layer forces. *J. Phys. Chem.* **1985**, *89*, 5180−5184.
(13) Komorowski, K.; Salditt, A.; Xu, Y.; Yavuz, H.; Brennich, M.; Jahn, R.; Salditt, T. Vesicle Adhesion and Fusion Studied by Small-Angle X-Ray Scattering. *Biophys. J.* **2018**, *114*, 1908−1920.
(14) Herrmann, L.; Johner, A.; Kékicheff, P. Interactions between Charged Lamellae in Aqueous Solution. *Phys. Rev. Lett.* **2014**, *113*, 268302.
(15) Schlaich, A.; dos Santos, A. P.; Netz, R. R. Simulations of Nanoseparated Charged Surfaces Reveal Charge-Induced Water Reorientation and Nonadditivity of Hydration and Mean-Field Electrostatic Repulsion. *Langmuir* **2019**, *35*, 551−560.
(16) Sonneville-Aubrun, O.; Bergeron, V.; Gulik-Krzywicki, T.; Jönsson, B.; Wennerström, H.; Lindner, P.; Cabane, B. Surfactant Films in Biliquid Foams. *Langmuir* **2000**, *16*, 1566−1579.
(17) Charitat, T.; Bellet-Amalric, E.; Fragneto, G.; Graner, F. Adsorbed and free lipid bilayers at the solid-liquid interface. *Eur. Phys. J. B* **1999**, *8*, 583−593.
(18) Daillant, J.; Bellet-Amalric, E.; Braslau, A.; Charitat, T.; Fragneto, G.; Graner, F.; Mora, S.; Rieutord, F.; Stidder, B. Structure and fluctuations of a single floating lipid bilayer. *Proc. Natl. Acad. Sci. U. S. A.* **2005**, *102*, 11639−11644.
(19) Hemmerle, A.; Malaquin, L.; Charitat, T.; Lecuyer, S.; Fragneto, G.; Daillant, J. Controlling interactions in supported bilayers from weak electrostatic repulsion to high osmotic pressure. *Proc. Natl. Acad. Sci. U. S. A.* **2012**, *109*, 19938−19942.
(20) Cubitt, R.; Fragneto, G. D17: the new reflectometer at the ILL. *Appl. Phys. A: Mater. Sci. Process.* **2002**, *74*, s329−s331.
(21) Crowley, T.; Lee, E.; Simister, E.; Thomas, R. The use of contrast variation in the specular reflection of neutrons from interfaces. *Phys. B* **1991**, *173*, 143−156.
(22) Koenig, B. W.; Krueger, S.; Orts, W. J.; Majkrzak, C. F.; Berk, N. F.; Silverton, J. V.; Gawrisch, K. Neutron Reflectivity and Atomic Force Microscopy Studies of a Lipid Bilayer in Water Adsorbed to the Surface of a Silicon Single Crystal. *Langmuir* **1996**, *12*, 1343−1350.
(23) Gerelli, Y. Aurore: new software for neutron reflectivity data analysis. *J. Appl. Crystallogr.* **2016**, *49*, 330−339.
(24) Malaquin, L.; Charitat, T.; Daillant, J. Supported bilayers: Combined specular and diffuse X-ray scattering. *Eur. Phys. J. E: Soft Matter Biol. Phys.* **2010**, *31*, 285−301.
(25) Fragneto, G.; Charitat, T.; Bellet-Amalric, E.; Cubitt, R.; Graner, F. Swelling of phospholipid floating bilayers: the effect of chain length. *Langmuir* **2003**, *19*, 7695−7702.
(26) Hishida, M.; Nomura, Y.; Akiyama, R.; Yamamura, Y.; Saito, K. Electrostatic double-layer interaction between stacked charged bilayers. *Phys. Rev. E: Stat. Phys., Plasmas, Fluids, Relat. Interdiscip. Top.* **2017**, *96*, 040601.
(27) Thurmond, R.; Dodd, S.; Brown, M. Molecular areas of phospholipids as determined by 2H NMR spectroscopy. Comparison of phosphatidylethanolamines and phosphatidylcholines. *Biophys. J.* **1991**, *59*, 108−113.
(28) Marsh, D. *Handbook of Lipid Bilayers*, 2nd ed.; Taylor & Francis, 2013.
(29) Fumagalli, L.; Esfandiar, A.; Fabregas, R.; Hu, S.; Ares, P.; Janardanan, A.; Yang, Q.; Radha, B.; Taniguchi, T.; Watanabe, K.; et al. Anomalously low dielectric constant of confined water. *Science* **2018**, *360*, 1339−1342.
(30) Parsegian, V. *Van der Waals Forces: A Handbook for Biologists, Chemists, Engineers, and Physicists*; Cambridge University Press, 2005.

DOI: 10.1021/acs.jpclett.9b02804
J. Phys. Chem. Lett. 2019, 10, 7195−7199